







Leveraging T cell co-stimulation for enhanced therapeutic efficacy of trispecific antibodies targeting prostate cancer

Yanping Sun , Linling Zhou , Xinyu Gu , Jiaqi Zhao , Jie Bi ,
Liqiang Pan 

To cite: Sun Y, Zhou L, Gu X, *et al.* Leveraging T cell co-stimulation for enhanced therapeutic efficacy of trispecific antibodies targeting prostate cancer. *Journal for ImmunoTherapy of Cancer* 2025;**13**:e010140. doi:10.1136/jitc-2024-010140

► Additional supplemental material is published online only. To view, please visit the journal online (<https://doi.org/10.1136/jitc-2024-010140>).

Accepted 21 February 2025



© Author(s) (or their employer(s)) 2025. Re-use permitted under CC BY-NC. No commercial re-use. See rights and permissions. Published by BMJ Group.

Department of Pharmacy, the Second Affiliated Hospital, School of Medicine and College of Pharmaceutical Sciences, Zhejiang University, Hangzhou, China

Correspondence to

Dr Liqiang Pan;
panliqiang@zju.edu.cn

ABSTRACT

Background Clinical trials have demonstrated the efficacy of bispecific antibodies in eliciting potent antitumor responses by redirecting T cells to target cancer cells, particularly for the treatment of hematologic malignancies. However, their efficacy against solid tumors is limited by intratumoral T-cell dysfunction and inadequate persistence. The co-stimulatory domains of 4-1BB, OX40, and CD28 are most widely used in engineering chimeric antigen receptor T-cells to augment T-cell responses.

Methods In this study, we designed three co-stimulatory trispecific T cell-engaging antibodies (TriTCEs) that target Prostate-specific membrane antigen, CD3, and an additional co-stimulatory receptor (OX40, 4-1BB, or CD28). We conducted comparative profiling of the attributes of distinct co-stimulatory signals to T-cell functions in prostate cancer models.

Results Co-stimulatory trispecific T-cell engagers enhance T-cell activation, proliferation, and display tumor cell-killing activity in vitro. These trispecific antibodies further boosted antitumor activity in humanized mouse xenograft models and increased the infiltration of CD45⁺ immune cells into solid tumors. Specifically, TriTCE-4-1BB and TriTCE-CD28 selectively promoted the expansion of effector memory T cells and increased the presence of CD4⁺ T cells more than TriTCE-OX40. T cells stimulated with TriTCE-4-1BB exhibited reduced exhaustion. Furthermore, T cells treated with co-stimulatory trispecific antibodies demonstrated enhanced metabolic activity characterized by increased oxidative phosphorylation and elevated glycolysis.

Conclusions Collectively, incorporating co-stimulatory receptor targeting domains represents a potentially effective strategy to unlock the full therapeutic potential of T-cell-engaging antibodies for the treatment of solid tumors.

INTRODUCTION

Over the last decade, advances in immunotherapy have revolutionized the paradigm of cancer treatment. Based on the generally accepted concepts of tumor immunosurveillance and tumor immunoediting, therapies such as chimeric antigen receptor T cells and

WHAT IS ALREADY KNOWN ON THIS TOPIC

⇒ Bispecific T-cell-engaging antibodies have shown clinical efficacy in hematologic malignancies. Their effectiveness against solid tumors, particularly cold tumors, is limited, possibly due to T-cell dysfunction and lack of persistence in the tumor microenvironment. Therapeutic strategies remain to be optimized to better confront the complex challenges posed by solid tumors.

WHAT THIS STUDY ADDS

⇒ We conducted a rigorous, side-by-side comparison of T-cell engager antibodies incorporating distinct co-stimulatory signals (4-1BB, CD28, and OX40) using a consistent structural framework and affinity profile. We highlight that distinct T-cell costimulation signals exert diverse effects on T-cell response dynamics. Specifically, we observed that TriTCE-4-1BB and TriTCE-CD28 costimulation preferentially expanded effector memory T cells and increased the presence of CD4⁺ T cells more than TriTCE-OX40. Additionally, this finding underscores the critical role of co-stimulatory signals in enhancing T-cell metabolic fitness, equipping them to withstand the demands of repeated antigen exposure in the tumor microenvironment.

HOW THIS STUDY MIGHT AFFECT RESEARCH, PRACTICE OR POLICY

⇒ This study provides important insights into the unique impact of T-cell-mediated immune regulation induced by distinct costimulation signals. It highlights the therapeutic promise of targeting T-cell costimulation pathways to enhance immune infiltration and efficacy in challenging solid tumor settings.

immune checkpoint receptor inhibitors that modulate immunoregulatory networks have made significant progress in controlling malignant diseases.^{1 2} Despite these promising anti-cancer responses, efficacy against otherwise “non-immunogenic” solid tumors, such as prostate, pancreatic, colorectal, and breast, has been modest or even negligible.³

Therefore, more effective treatments are needed to optimize T cell-mediated antitumor immunity and extend the benefits of immunotherapy to a broader range of patients.

Bispecific T-cell engagers (TCEs) offer an appealing approach by redirecting T cells to tumor cells through dual binding: one arm targets a tumor-associated antigen on the cancer cell, while the other binds to the CD3 complex on T cells, resulting in T-cell-mediated tumor cell lysis.⁴ Trispecific TCEs build on this foundation by incorporating an additional specificity, allowing them to engage multiple targets or immune pathways. This advancement provides a more nuanced approach to immunotherapy, potentially enhancing the robustness of the antitumor response. Despite the rapid increase in the number of clinical trials of bispecific TCEs, clinical benefits for solid tumor treatment have yet to be demonstrated. Barriers to solid tumor treatment include lack of universal tumor-specific targets, extensive tumor heterogeneity, and the complex tumor microenvironment (TME).⁵ Highly immunosuppressive TMEs could lead to T-cell dysfunction and exhaustion within the tumor.^{6,7} Therefore, enhancing and sustaining T-cell function in the TME is crucial for advancing T-cell engager strategies against solid tumors.

During the initiation of the T-cell immune response, co-stimulation synergizes with TCR signaling and enables T cells to respond to their environment, rescuing activated T cells from anergy. CD28 was one of the first co-stimulatory receptors identified to mediate downstream signaling following TCR activation, leading to T-cell activation, clonal expansion, and differentiation.⁸ Co-stimulatory receptors of the Tumor Necrosis Factor Receptor Superfamily (TNFRSF), such as OX40 (TNFRSF4) and 4-1BB (TNFRSF9), have also been extensively studied and are particularly interesting targets for cancer treatment.^{9,10} These receptors differ in their expression pattern and timing of action. CD28 is constitutively expressed on both resting and activated T cells and is involved in the initial activation phase of the immune response. In contrast, OX40 and 4-1BB are not expressed on resting T cells, but can be upregulated on T-cell activation, particularly during the later stages of the immune response. Engagement of these immune co-stimulators by ligands or agonistic antibodies promotes T-cell proliferation, cytolytic effector functions, and protects lymphocytes from programmed cell death.^{11,12} Early attempts to develop potent agonists of co-stimulatory molecules have resulted in unacceptable clinical toxic effects. For instance, a phase I clinical trial of a superagonist anti-CD28 antibody (TGN1412) resulted in an unexpected life-threatening cytokine-release syndrome.¹³ In another case, trials with an anti-4-1BB agonistic mAb (urelumab) were terminated because of severe hepatotoxicity risks.¹⁴ The effect of agonistic mAbs is not spatially restricted to the tumor; thus, peripheral toxicities may reduce the therapeutic window for agonist therapies, which limits their antitumor efficacy.

To achieve improved targeting and signal transduction to sustain T-cell immune responses against such solid tumors, we developed prostate-specific membrane antigen (PSMA)-targeted T cell-engaging trispecific antibodies, which redirected T cells specifically to cancer cells and delivered co-stimulation signals simultaneously. Here, we focused on OX40, 4-1BB, and CD28 co-stimulation. In this study, we found that these trispecific antibodies activated T cells with improved tumor cell-killing efficacy *in vitro* and enhanced antitumor response in peripheral blood mononuclear cells (PBMCs)-engrafted NOD CRISPR Prkdc Il2r gamma (NCG) triple-immunodeficient mouse models. Furthermore, we found that co-stimulatory TriTCEs mediated T-cell metabolic fitness and led to mitochondrial biogenesis. Collectively, these data suggest that the combination of tumor-targeted T-cell engaging and co-stimulation signals into one format of trispecific antibodies may provide a potential immunotherapy strategy to boost immune responses against solid tumors.

METHODS

Cells

The prostate cancer cell lines LNCaP, 22Rv1, and C4-2B were gifted by Prof. Dan Li at Zhejiang University. Cells were cultured in RPMI-1640 (Gibco) supplemented with 10% FBS (Gibco) and 1% penicillin/streptomycin solution (Solarbio). Human PBMCs from healthy donors were purchased from Sailybio. Cells were maintained in a humidified chamber at 37°C with 5% CO₂. The reagent sources and catalog numbers are listed in online supplemental table S2.

Expression and purification of antibodies

The variable regions of the PSMA-targeting Fab were derived from the J591 monoclonal antibody.¹⁵ Variable regions of the CD3-targeting Fab were derived from the humanized OKT3 monoclonal antibody.¹⁶ The anti-human OX40, 4-1BB, and CD28 scFv sequences were cloned from 11D4, hu107.1x, and TGN1412, respectively.^{17–19} All expression plasmids were synthesized by GenScript and purified using plasmid extraction kits (Tiangen). Antibodies were produced by Expi293 cells (ThermoFisher) using 1 mg/mL optimized linear polyethylenimine reagent (Yeasen Biotechnology) for plasmid transfection. Supernatants were harvested, clarified, and purified using nickel chromatography (GE Healthcare) and anti-FLAG M1 Agar Affinity Gel (Millipore Sigma). Purified proteins were concentrated in sterile phosphate-buffered saline (PBS) by ultrafiltration using an Amicon Ultra 50 kDa device (Merck), and protein concentrations were measured using NanoDrop One (ThermoFisher). Purified proteins were resolved on a 10% Tris-glycine SDS-PAGE gel under reducing conditions (5% β-mercaptoethanol), followed by Coomassie Blue staining. The purified antibodies were stored in aliquots at –80 °C.

Cell binding

The binding of the antibodies to PSMA⁺ cells was analyzed by flow cytometry. Cells were harvested, washed with flow

cytometry buffer (PBS, 1% BSA), and incubated with the corresponding antibody for 30 min on ice. After incubation, the cells were washed twice and resuspended in a 1:100 diluted solution of FITC-conjugated anti-human IgG antibody (Beyotime), and incubated for 30 min on ice in the dark. The cells were then washed twice and resuspended in flow cytometry buffer. The mean fluorescence intensity (MFI) was measured using ACEA Novo-Cyte (ACEA Biosciences). The binding of antibodies to human CD3 was assessed in Jurkat cells. A bio-layer interferometry experiment was conducted by Hisun Pharmaceutical (Zhejiang, China)

T-cell activation and proliferation assays

The target tumor cells were seeded (50,000 cells/well) in a 48-well plate and incubated overnight, followed by co-culture with human PBMCs at an effector-to-target (E:T) ratio of 4:1 with serially diluted antibodies for 48 hours. The cells were pelleted and stained with fluorophore-conjugated antibodies against CD4, CD8, CD69, and CD25 and analyzed by flow cytometry. For T-cell proliferation analysis, tumor cells and PBMCs were co-cultured as described above. PBMCs were labeled with 1 μ M CellTrace CFSE (ThermoFisher). The proliferation rate was measured as the percentage of divided T cells that showed a decrease in the CFSE signal compared with the untreated control. For the blocking experiments, specific receptor proteins were used to selectively inhibit the interaction between the TriTCEs and their respective receptors on T cells. The proteins, sourced from Acrobiosystems, are listed in online supplemental table S2. TriTCEs (100 pM) were preincubated with the corresponding blocking proteins at a titrated concentration for 1 hour at 37°C in a 5% CO₂ incubator. T cells were isolated from human PBMCs using the EasySep Human T Cell Isolation Kit (STEMCELL Technologies). Following preincubation, the T cells were co-cultured with target tumor cells (LNCaP) in the presence of TriTCEs and the blocking proteins. Cells were cultured for an additional 24–72 hours, after which T-cell activation and proliferation assays were performed.

Cytotoxicity and cytokine secretion assays

Prostate tumor cells were seeded (10,000 cells/well) in 96-well plates and incubated overnight, followed by incubation with human PBMCs at an E:T ratio of 1:1, 2:1, and 4:1 in the presence of diluted antibodies for 48 hours. Cellular cytotoxicity was quantified according to the manufacturer's instructions (Cytotoxicity LDH Assay Kit-WST, Dojindo) (LDH, lactate dehydrogenase).

For cytokine analysis, cell culture supernatant was harvested and quantified using Human IL-2, Human TNF- α ELISA MAX Deluxe (BioLegend), and IFN gamma Human ELISA Kit (ThermoFisher).

T-cell phenotype analysis assays

In the exhaustion phenotype analysis assays, LNCaP cells and human PBMCs were co-cultured at a low E: T ratio

of 1:1 in the presence of 10 ng/mL TGF- β and IL-10 and treated with 10 nM antibodies. Cells were collected after 48 hours and stained with fluorophore-conjugated anti-human CD4, CD8, PD-1, and TIM-3 antibodies (BioLegend), and then analyzed by flow cytometry.

For T-cell memory subtype analysis, LNCaP cells and human PBMCs were co-cultured with 1 nM antibodies as described above for 7 and 14 days and analyzed by flow cytometry for the following T-cell subsets: naïve (CCR7⁺CD45RO⁻), T_{CM} (CCR7⁺CD45RO⁺), T_{EM} (CCR7⁻CD45RO⁺), and Treg (CD4⁺Foxp3⁺CD25^{hi}).

In vitro multiround co-culture assay

Tumor cells labeled with CFSE were seeded in 48-well plates at a density of 2×10^5 cells per well 1 day before the addition of human PBMCs. PBMCs were added at an E:T ratio of 1:1 without the addition of exogenous cytokines. Four, three, and two plates were performed for the first, second, and third rounds of co-culture, respectively. At the end of each round of co-culture, one plate was collected to quantify residual tumor cells (CFSE-labeled) and T cells by flow cytometry. Dead cells were excluded using Zombie Aqua Dye (BioLegend). On days 3, 6, and 9, cells were collected and transferred into a new well in which 2×10^5 tumor cells were seeded 1 day before adding cells for the next round of co-culture. For the final round of the co-culture experiment, the expression of Granzyme B, Ki67, and Bcl-xL were determined by intracellular flow staining using the Intracellular Fixation & Permeabilization kit (ThermoFisher).

In vivo efficacy studies in NCG mouse xenograft models

Male immunodeficient NCG mice aged 6–8 weeks were purchased from GemPharmatech. For the 22Rv1 mCRPC xenograft model, NCG mice (n=5) were subcutaneously implanted with 5×10^6 22Rv1 tumor cells (day 0). When the tumors reached approximately 60 mm³, the mice were intravenously engrafted with 7×10^6 human PBMCs per animal 1 day before the start of treatment. Mice were randomized into groups and received treatment with TriTCEs, BiTCE (2.5 μ g/dose; adjusted to equimolar concentration based on molecular weight), or vehicle (intravenous) every 3 days for a total of five doses. In a follow-up study, five cohorts of NCG mice (n=5) were engrafted with 5×10^6 22Rv1 tumor cells. T cells were isolated from PBMCs using the EasySep Human T Cell Isolation Kit (STEMCELL Technologies). T cells were injected 1 day before treatment began. Treatments were described as above. Treatments in the advanced model were initiated when the tumor size was approximately 200 mm³. The tumor burden was monitored twice a week using a caliper, and the study was terminated when the tumor volume exceeded 1500 mm³. After termination of the in-life portion of the study, serum samples from the mice were collected to test AST, ALT, CREA, and BUN levels (AST, aspartate aminotransferase; ALT, alanine aminotransferase; CREA, creatinine; BUN, blood urea

nitrogen). Animals had free access to food and sterile water.

Metabolic assays

T-cell metabolism was measured using a Seahorse XFe96 analyzer (Seahorse Bioscience). Individual wells of an XF96 cell-culture microplate were coated with poly-L-lysine. The matrix was allowed to adsorb for 20 min at room temperature, aspirated, and air-dried for at least 2 hours until use. Next, 2×10^5 /well sorted T cells treated with TriTCEs or BiTCE were seeded onto 96-well Seahorse XF-96 assay plates in Seahorse RPMI medium with additives. The microplate was centrifuged at $200 \times g$ for 1 min and the cells were incubated at 37°C in a non- CO_2 incubator for 45 min. Oxygen consumption and extracellular acidification rates (ECARs) were automatically calculated and recorded using Seahorse XF-96 software. Cellular oxygen consumption rate (OCR) was measured under basal conditions and following treatment with 1 μM oligomycin, 1.5 μM FCCP, and 0.5 μM rotenone/antimycin A (XF Cell Mito Stress kit, Seahorse Bioscience). Cellular ECAR was measured under basal conditions and following treatment with 10 mM glucose, 1 μM oligomycin, and 50 mM 2-DG (XF Cell Glycolysis Stress kit, Seahorse Bioscience).

RNA-seq analysis

Total RNA was extracted from sorted $\text{CD}3^+$ T cells by flow cytometry using TRIzol reagent (Invitrogen, California, USA). Messenger RNA libraries were prepared (VAHTS Universal V6 RNA-seq Library Prep Kit) and sequenced on the Illumina Novaseq 6000 platform using paired-end 150 bp reads, with 52 million reads on average (range, 51–54 million). Transcriptome sequencing and analysis were conducted by OE Biotech (Shanghai, China). Differential expression analysis was performed using DESeq2.²⁰ Gene Set Enrichment Analysis (GSEA) was performed using GSEA software.²¹ Pathway gene sets were downloaded from Molecular Signature Database.

Statistical analysis

Graph generation and statistical analysis were performed using GraphPad Prism V.9 software, and data are presented as mean \pm SD. Statistical differences between mean values were determined using unpaired two-tailed Student's t-test or one-way analysis of variance with Dunnett's post-test analysis as indicated in figure legends, * $p < 0.05$, ** $p < 0.01$, *** $p < 0.001$, **** $p < 0.0001$. Survival curves were analyzed by log-rank test. In all cases, a significant result was defined as a $p < 0.05$.

RESULTS

Co-stimulatory TriTCEs enhance T-cell activation, cytokine secretion, and tumor cell cytotoxicity in vitro

To evaluate the effects of T-cell co-stimulation provided by different co-stimulatory receptors, we engineered a variety of trispecific T-cell-engager antibody constructs.

All constructs were combinations of anti-human PSMA and anti-human $\text{CD}3\epsilon$ (signal 1) variable fragments fused into the hIgG1 isotype and contained one of the anti-human OX40/4-1BB/ $\text{CD}28$ (signal 2) scFvs connected with flexible five-amino-acid (G_4S) linkers into the C-terminus of the Fc domain (figure 1A,B). These novel antibodies were designated TriTCE-OX40, TriTCE-4-1BB, and TriTCE- $\text{CD}28$, respectively. Reduced SDS-PAGE was used to validate the antibodies by visualizing the expected subunits (online supplemental figure S1). Next, the specific cell binding of TriTCEs and BiTCE to PSMA^+ tumor cell lines was confirmed by flow cytometry. TriTCEs and BiTCE bound to Jurkat cells expressing human $\text{CD}3$, as determined by flow cytometry (figure 1C). The binding affinities of TriTCE-OX40, TriTCE-4-1BB, and TriTCE- $\text{CD}28$ to their respective co-stimulatory receptors were determined to be in a similar range, with equilibrium dissociation constants (K_D) of 2.765 nM, 1.655 nM, and 5.547 nM, respectively (figure 1C and online supplemental table S1).

To assess the T-cell activation activity of these TriTCEs, we investigated the upregulation of $\text{CD}69$ and $\text{CD}25$ in T cells co-cultured with LNCaP (PSMA^+) tumor cells in the presence of increasing concentrations of antibodies. We observed that TriTCEs induced dose-dependent activation of both $\text{CD}4^+$ and $\text{CD}8^+$ T cells, comparable to the BiTCE (figure 1D). The EC_{50} values for TriTCE-OX40, TriTCE-4-1BB, and TriTCE- $\text{CD}28$ mediated $\text{CD}8^+$ T cell $\text{CD}69$ upregulation were 0.59 pM, 0.01 pM, and 0.27 pM, respectively. Furthermore, the TriTCE- $\text{CD}28$ group showed superior T-cell activation in terms of the maximum percentage of $\text{CD}25$ upregulation, ranging from 71.38% to 76.59%. Following a 72-hour incubation, TriTCE-mediated T-cell proliferation was assessed by incubating CFSE-labeled PBMC cells with tumor cells. After incubation with BiTCE, TriTCE-OX40, TriTCE-4-1BB, and TriTCE- $\text{CD}28$, the no-expansion T-cell ratio was 67.76%, 56.65%, 56.42%, and 51.60% for $\text{CD}4^+$ T cells, and 50.93%, 47.99%, 46.90%, and 46.30% for $\text{CD}8^+$ T cells (figure 2A). To assess whether antibody stimulation leads to the upregulation of inducible co-stimulatory receptor expression, T cells were co-cultured with tumor cells in the presence of corresponding antibodies for 4, 24, and 48 hours. We observed an upregulation of 4-1BB and OX40 expression on T cells following antibody treatment, and it became more pronounced over time, indicating a dynamic activation response to the stimuli (online supplemental figure S2). To further validate the roles of these co-stimulatory signals, we conducted additional blocking experiments to assess the contributions of the OX40, 4-1BB, and $\text{CD}28$ signaling pathways. In the blocking experiments, we observed a dose-dependent inhibition of T-cell activation and proliferation with increasing concentrations of blocking proteins, underscoring the importance of co-stimulatory signals triggered by TriTCEs (online supplemental figure S3 and S4).

To determine the cytolytic effect of the TriTCEs, we performed a series of tumor cell-killing cytotoxicity

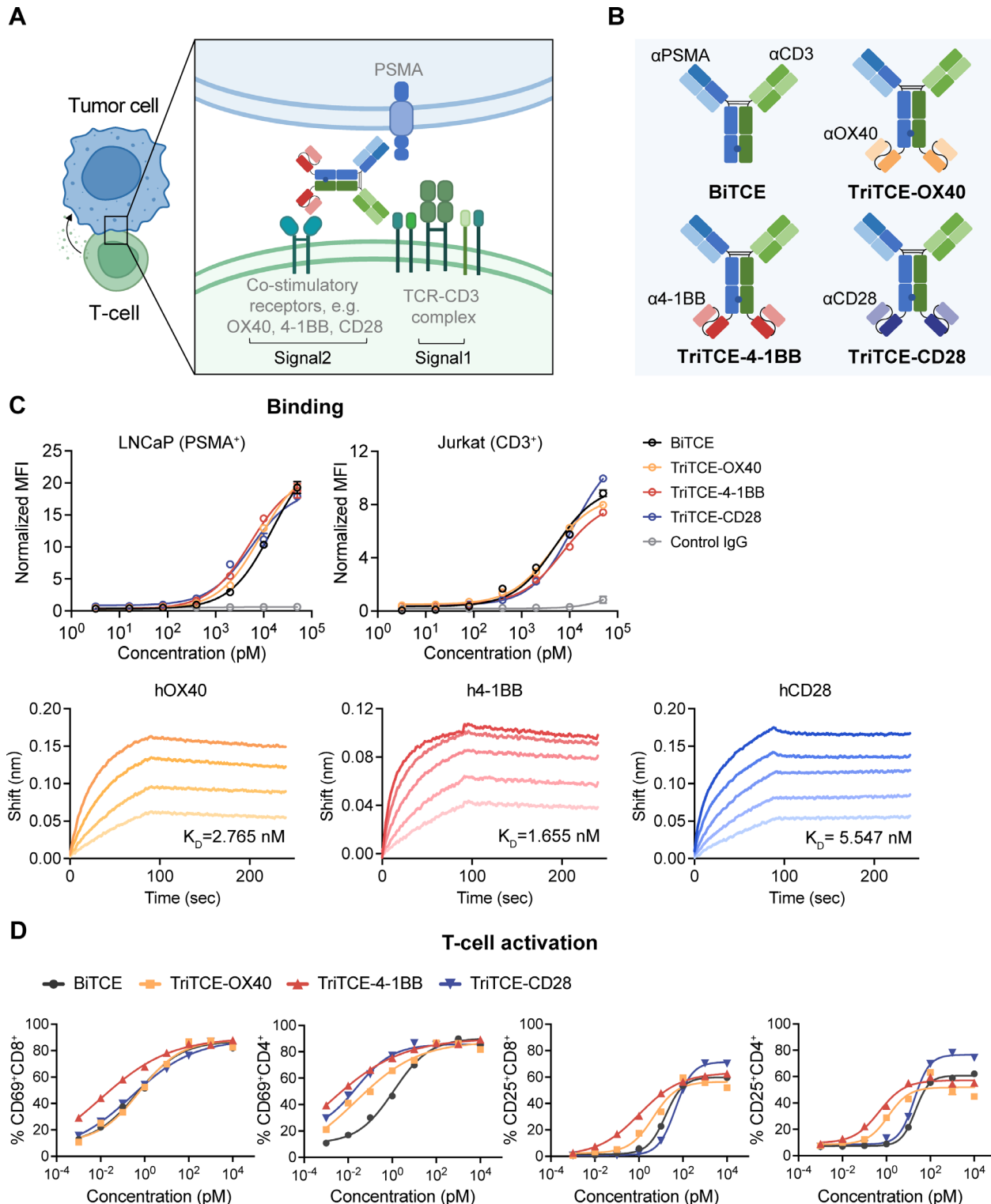


Figure 1 Schematic design of co-stimulatory TriTCEs. (A) Schematic representation of T cells targeting tumor cells via co-stimulatory T-cell-engaging antibody, initiating antitumor immune responses. (B) Schematic diagram showing the bispecific antibody and trispecific antibodies constructed for this study (blue, anti-human PSMA Fab; green, anti-human CD3 Fab; orange, anti-human OX40 single-chain variable fragment (scFv); red, anti-human 4-1BB scFv; purple, anti-human CD28 scFv). (C) Top: Flow cytometric analysis of antibody binding to the PSMA-expressing tumor cell line (LNCaP) and CD3-expressing cell line (Jurkat) ($n=3$). Bottom: Determination of binding affinities of TriTCE-OX40 to human OX40, TriTCE-4-1BB to human 4-1BB, and TriTCE-CD28 to human CD28 using BLI. K_D values (equilibrium dissociation constants) are indicated ($n=3$). (D) CD69 and CD25 upregulation were assessed on CD8⁺ and CD4⁺ T cells by flow cytometry in co-cultures of human PBMCs and LNCaP (PSMA positive) target tumor cells in a 4:1 ratio in the presence of increasing concentrations of BiTCE, TriTCE-OX40, TriTCE-4-1BB, and TriTCE-CD28 for 48 hours ($n=3$). Data are representative of three independent experiments. BLI, bio-layer interferometry; PSMA, prostate-specific membrane antigen; TriTCEs, trispecific T cell-engaging antibodies.

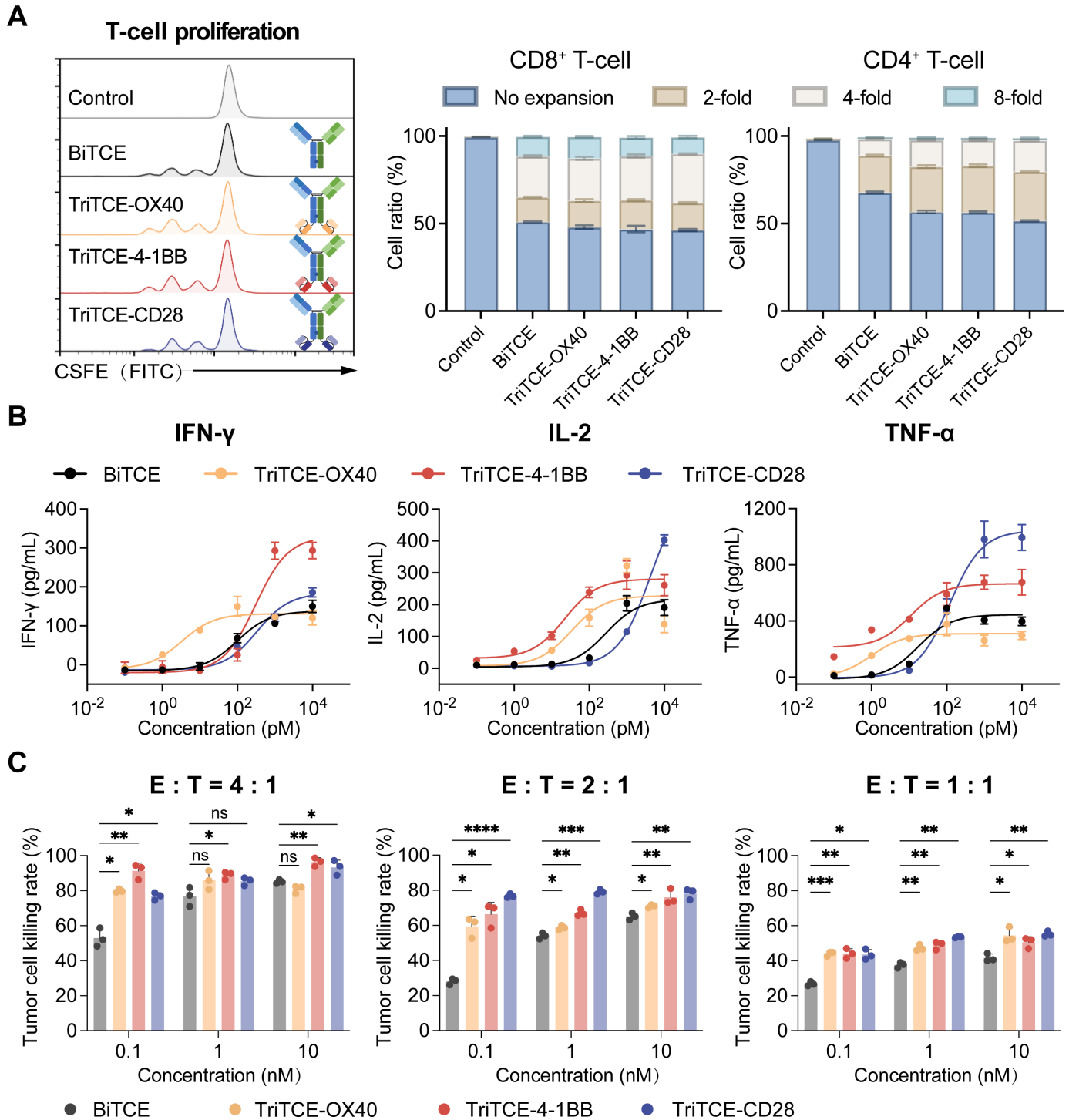


Figure 2 Costimulatory TriTCEs enhance T-cell proliferation, cytokine secretion, and tumor cell cytotoxicity in vitro. (A) Proliferation of CFSE-labeled CD8⁺ and CD4⁺ T cells was evaluated following co-culture with PBMCs and LNCaP cells in the presence of 1 nM antibody for 72 hours (effector:target (E:T) ratio of 4:1). (B) IFN- γ , IL-2, and TNF- α production were measured by ELISA in culture supernatants from incubation of PBMC and LNCaP cells in a 4:1 ratio treated with increasing concentrations of BiTCE, TriTCE-OX40, TriTCE-4-1BB, and TriTCE-CD28 for 48 hours. (C) Cytotoxicity of the PSMA⁺ tumor cell line LNCaP with trispecific antibodies and the bispecific control was assessed using the cytotoxicity LDH assay kit in vitro at effector:target ratio of 4:1, 2:1, 1:1. Data show mean \pm SD (n=3 independent experiments each) and were analyzed by one-way ANOVA with Dunnett's post-test analysis. *p<0.05; **p<0.01; ***p<0.001; ****p<0.0001; ns, no significance compared with the bispecific control. ANOVA, analysis of variance; PBMCs, peripheral blood mononuclear cells; TriTCEs, trispecific T cell-engaging antibodies; LDH, lactate dehydrogenase; CFSE, carboxyfluorescein succinimidyl ester.

evaluation assays. We analyzed the production of effector molecules from co-culture supernatants. TriTCEs mediated the release of IFN- γ , IL-2, and TNF- α from T cells at levels comparable to those in the bispecific control (figure 2B). The effector-to-target (E:T) cell ratio appears to correlate with the shaping of the T-cell immune responses and cytolytic activity towards cancer cells. We examined the cytotoxicity of TriTCEs at multiple E:T ratios. TriTCEs showed potent tumor cell killing at a low E:T ratio (1:1), with an average maximum tumor killing of 50.49%–55.24% (figure 2C). We also observed TriTCE-mediated cytotoxicity in other prostate cancer cell lines, 22Rv1 and C4-2B (online supplemental figure S5A and S5B). Although we observed some level of antigen-independent activation (online supplemental figure S6), TriTCEs and BiTCE exhibited minimal cytotoxic activity against antigen-negative tumor cells PC-3 in the same E:T co-culture experiment, which was also observed in another PSMA-negative DU145 tumor cells, indicating the selective antigen-dependent cytotoxicity (online supplemental figure S7). Additionally, to mimic an immunosuppressive environment, we assessed the cytotoxicity of TriTCEs in a co-culture with exogenous IL-10 and TGF- β , which are known inhibitory cytokines.²² The addition of IL-10 and TGF- β reduced cytotoxicity mediated by T-cell engagers, while the reduction in tumor cell lysis rate in the TriTCE groups was significantly less pronounced than that in the bispecific control. In the presence of 10 nM BiTCE, TriTCE-OX40, TriTCE-4-1BB, and TriTCE-CD28, 25.40%, 39.39%, 35.66%, and 39.76% cytotoxicity rates, respectively, were observed at 10 ng/mL IL-10/TGF- β dose at 1:1 E:T ratio (online supplemental figure S5C). These data suggest that co-stimulatory TriTCEs may restore T-cell effector function against tumor cells in an immune-cold TME.

Co-stimulatory TriTCEs increase sustained T-cell function under repeated tumor stimulation

Repetitive antigen stimulation or tonic receptor signaling may result in rapid T-cell exhaustion, which limits anti-tumor immune response.²³ We hypothesized that co-stimulation signals via TriTCEs might support T cells to overcome activation-induced cell death and maintain functional sustainability under repeated tumor stimulation. Therefore, we performed multi-round co-culture experiments to model chronic antigen exposure in vivo and analyzed the number of tumor cells and T cells. All TriTCE treatment groups showed significantly fewer live residual tumor cells in the last three rounds, whereas the TriTCE-OX40 group showed less efficacy than the other two TriTCEs (figure 3A). After four rounds of continuous antigen stimulation, the TriTCE-CD28 group exhibited the highest CD3⁺ T-cell counts, followed by the TriTCE-4-1BB group (figure 3B), despite the same number of input PBMCs seeded at the beginning of the co-culture assays, indicating that co-stimulation signals potentially induced rapid clonal expansion.

We examined the functional phenotype of T cells in the different groups using flow cytometry. T cells in the TriTCE group displayed an effector phenotype with cytolytic capacity, as indicated by the elevated expression of CD107a and granzyme B (figure 3C,D). Furthermore, T cells treated with TriTCEs maintained their proliferative advantage over T cells in the bispecific control in the final round of the tumor stimulation cycle (as measured by Ki67, figure 3E).

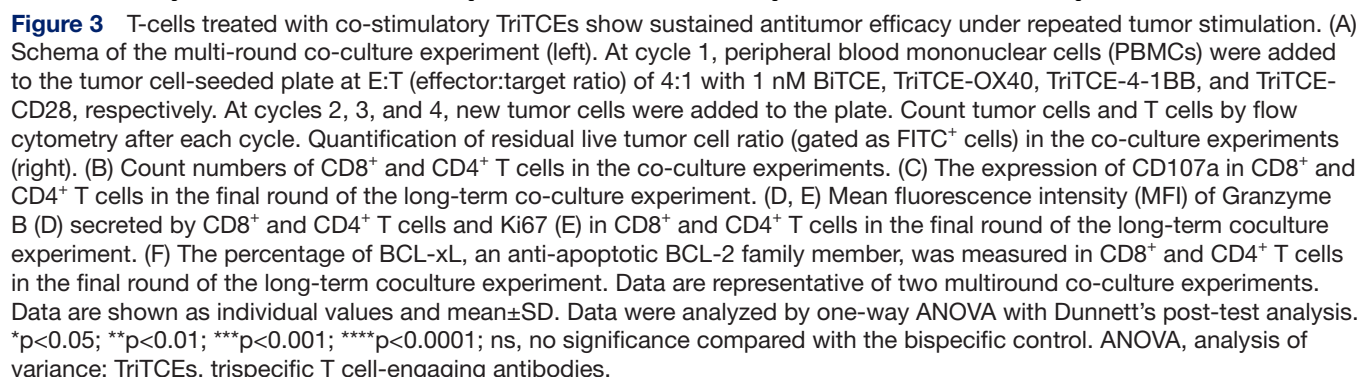
To study whether co-stimulatory signals through TriTCEs could affect the survival of T cells, we assessed their effect on the anti-apoptotic protein Bcl-xL, which was previously reported to be involved in the cell survival pathway. As shown in figure 3F,T cells showed elevated Bcl-xL expression after incubation with TriTCEs, as measured by intracellular staining in primary human CD4 and CD8 cells. Altogether, these results suggest that T cells stimulated with TriTCE have improved persistence under continuous antigen stimulation, with maintained cytolytic activity. T cells treated with co-stimulatory TriTCEs were less prone to apoptosis, suggesting that these cells may have better persistence potential and contribute effectively to the fight against tumor cells.

Co-stimulatory TriTCEs inhibit tumor progression in NCG mouse xenograft models

We used NCG mouse xenograft models to evaluate whether co-stimulation of distinct signaling pathways provided by TriTCEs could enhance antitumor efficacy in vivo. In the first tumor model, immunodeficient NCG mice were subcutaneously transplanted with 22Rv1 prostate cancer cells into the right flank and engrafted with resting human PBMCs. Compared with the vehicle treatment and the BiTCE control group, TriTCEs significantly inhibited the growth of 22Rv1 mCRPC xenograft tumors at doses as low as 100 μ g/kg (figure 4A). Furthermore, tumor growth inhibition (TGI; %) in the TriTCE-OX40, TriTCE-4-1BB, and TriTCE-CD28 groups reached 53.3%, 66.1%, and 56.3% at the end of the study, respectively, compared with the BiTCE control (figure 4A).

To further investigate the antitumor activity of TriTCEs in an advanced mCRPC tumor model, the antibody treatment was delayed until the tumors reached approximately 200 mm³. Although the antitumor efficacy was reduced due to the large tumor burden, the TriTCE treatment groups still exhibited a better antitumor response and longer overall survival, with superior efficacy in TriTCE-4-1BB-treated mice (figure 4B,D). The mouse body weight and serum biochemical indicators remained stable throughout the treatment period (figure 4E and online supplemental figure S8).

In a follow-up study, to verify the important role of the T-cell population in tumor regression, mice were transplanted with purified and preactivated human CD3 T cells and were administered intravenously with TriTCEs and a BiTCE control at the same doses as in the first study. The tumor growth inhibition (TGI) rates for TriTCE-OX40, TriTCE-4-1BB, and TriTCE-CD28 were 35.3%, 51.1%,



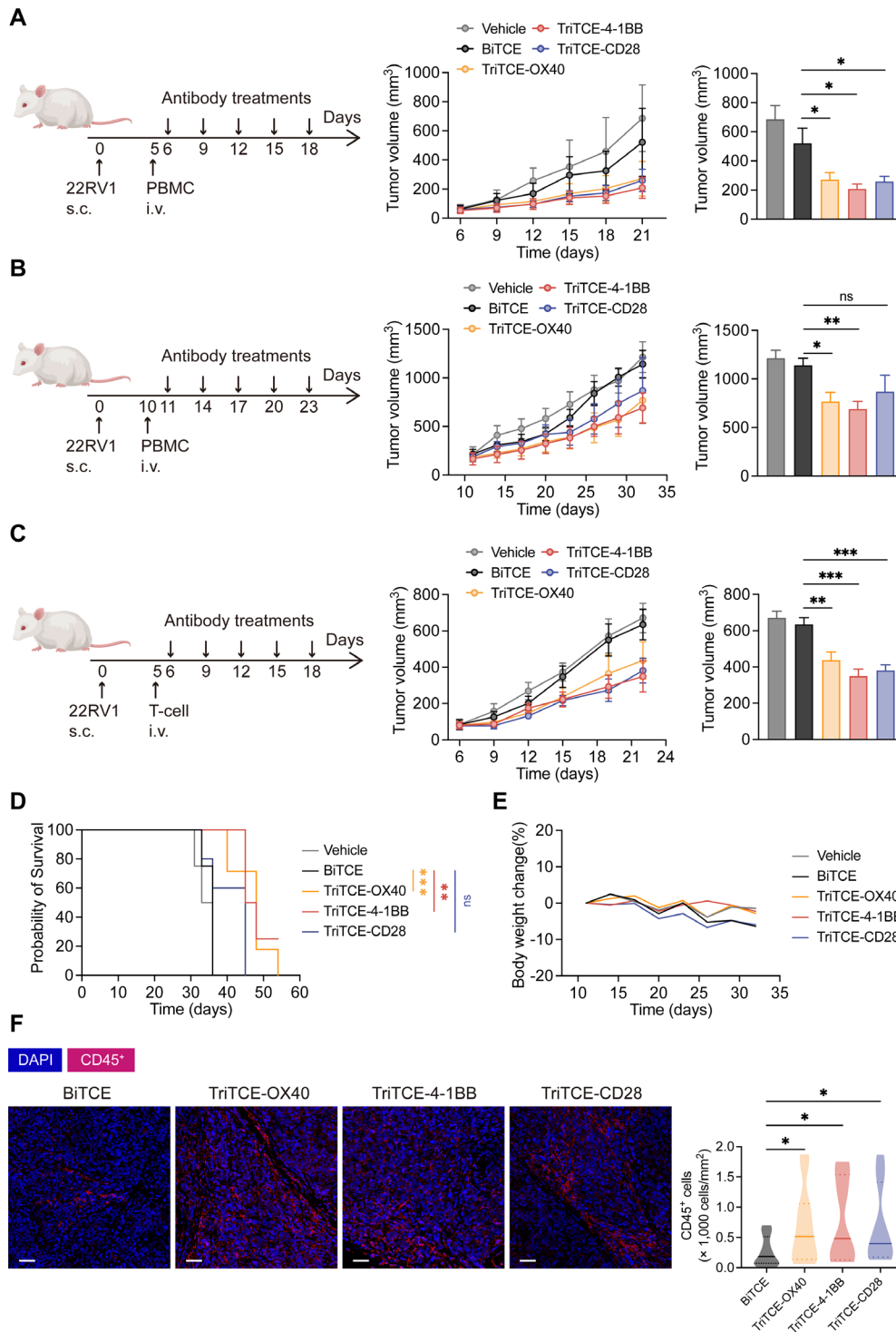


Figure 4 Co-stimulatory TrITCEs inhibit tumor progression in NCG mouse xenograft models. (A) Schematic diagram of the experimental design. NCG mice (NOD/ShiLtJGpt-*Prkdc*^{em26Cd52}*Il2rg*^{em26Cd22}/Gpt) were engrafted with 5×10^6 22Rv1 tumor cells to establish the prostate xenograft model ($n=5$ mice per group). 7×10^6 human PBMCs were inoculated, and every 3 days antibody treatment began when the average tumor volume was ~ 60 mm³. Tumor burden was quantified at various time points. (B) Tumor growth inhibition was evaluated in advanced 22Rv1 tumor-bearing mice. Treatment began when the average tumor volume was ~ 200 mm³ ($n=5$ mice per group). (C) Tumor growth inhibition was evaluated in 22Rv1 tumor-bearing mice using CD3⁺ T cells as effector cells ($n=5$ mice per group). (D) Overall survival curves of advanced tumor-bearing mice following antibody treatment therapy. (E) Representative body weight variation of different treatment groups. (F) Tumors were collected at the end of the study, and immunofluorescence was performed for human CD45⁺ cells. Representative images for each treatment group and quantification of positively stained cells are shown. Scale bars represent 50 μ m. Data show mean \pm SD and were analyzed by two-way ANOVA with Dunnett's post-test analysis. (A–C) or unpaired, two-tailed Student's *t*-test (F). Differences between survival curves (D) were analyzed by log-rank test. * $p < 0.05$; ** $p < 0.01$; *** $p < 0.001$; ns, no significance compared with the bispecific control. ANOVA, analysis of variance; TrITCEs, trispecific T cell-engaging antibodies.

and 44.9% at the end of the study, respectively, compared with the BiTCE control treatment (figure 4C), demonstrating the cytotoxic function of the T-cell population induced by TriTCEs. Immunofluorescence analysis of the harvested tumors revealed substantial immune cell infiltration in tumors of TriTCE-treated mice, whereas the BiTCE-treated mice had low detectable TILs (figure 4F). Overall, these data indicated that TriTCEs with co-stimulatory signals promoted antitumor effects in mCRPC prostate cancer xenograft models *in vivo*.

Co-stimulatory TriTCEs induce distinct phenotypes on tumor antigen stimulation

To evaluate the mechanism of action of these co-stimulatory TriTCEs, we compared the proportions of CD4 and CD8 subtypes among the proliferated T cells co-cultured with tumor cells in the presence of the indicated TriTCEs and BiTCE. Interestingly, following a single stimulation, TriTCE-OX40 treatment preferentially expanded the CD8⁺ T-cell population, while TriTCE-4-1BB and TriTCE-CD28 treatments expanded the CD4⁺ T-cell population (figure 5A and online supplemental figure S9). The cells were pre-gated for CD3⁺ T-cells.

The immunosuppressive TME can cause T cell exhaustion and limit immune responses in the treatment of solid tumors.²⁴ Therefore, we investigated whether the co-stimulatory signal induced by TriTCEs could attenuate the exhaustion of T cells in the TME in the presence of the immunosuppressive cytokines IL-10 and TGF- β . We analyzed the expression of T-cell exhaustion markers, including PD-1 and TIM-3, on CD4⁺ and CD8⁺ T cells using flow cytometry in a co-culture experiment at a low E: T ratio of 1:1. As shown in figure 5B, the frequencies of PD-1 and TIM-3-positive cells in both CD4⁺ and CD8⁺ T cells treated with TriTCE-4-1BB were the lowest among the three TriTCE groups.

Next, to determine the differentiated T-cell pool in the long-term co-culture system, we analyzed the memory phenotype of expanded T cells *in vitro* on days 7 and 14. We assessed the expression of CD45RO and CCR7 cell surface markers associated with T-cell memory differentiation. After stimulation with TriTCEs, the proportion of CD45RO⁺CCR7⁻ effector-memory cells progressively increased over time. Notably, CD8⁺ T-cells in the TriTCE-CD28 group yielded a higher proportion of the effector-memory phenotype faster, at day 7 (figure 5C,E), in contrast to the TriTCE-OX40 group, which maintained a high frequency of CD45RO⁺CCR7⁺ central memory CD4⁺ T-cell population. By day 14, the TriTCE-4-1BB and TriTCE-CD28 groups showed higher enrichment of the CD45RO⁺CCR7⁻ effector memory CD8⁺ T-cell population than the BiTCE group (figure 5E).

Overexpansion of Tregs, an immunosuppressive T cell subset, may potentially suppress the antitumor response.²⁵ Analysis of the expanded CD4⁺ T cell subset revealed a relatively lower proportion of CD25⁺Foxp3⁺ CD4⁺ Treg cells in the TriTCE-OX40 group (figure 5D).

Co-stimulatory TriTCEs potentiated T-cell metabolic fitness

We speculated that specific signals from the co-stimulatory signaling domain in the antibody structure supported T-cell mitochondrial biogenesis, thus endowing these cells with greater mitochondrial mass. Using flow cytometry, we measured the mitochondrial mass in CD3⁺ T cells by staining the cells with MitoTracker Green. Our results revealed a significantly increased mitochondrial mass in T cells treated with these trispecific antibodies (figure 6B). Additionally, compared with the BiTCE group, we observed an upregulation of mitochondrial membrane potential in T cells co-cultured with target tumor cells, indicating augmented mitochondrial respiration on antigen stimulation (figure 6A,C). To further characterize the metabolic regulatory effect of co-stimulatory trispecific antibodies in T cells, we analyzed the metabolic profiles of sorted CD3⁺ T cells using Seahorse assays. To mimic persistent tumor antigen stimulation in the TME, we established a multiround co-culture system of target tumor cells and CD3⁺ T cells (figure 6D). Notably, both basal and maximal OCR of sorted CD3⁺ T cells were markedly elevated on trispecific antibody treatment, providing evidence that co-stimulatory signals actively reprogram T cell metabolism towards a higher oxidative phosphorylation (OXPHOS) state (figure 6E). We also measured the ECAR, which represents cell glycolytic activity, as a measurable surrogate for lactic acid production during glycolysis. We found that T cells stimulated with trispecific antibodies showed elevated glycolytic activity compared with those treated with bispecific antibodies poststimulation (figure 6F). Enhanced glycolysis observed in T cells stimulated with co-stimulatory trispecific antibodies did not disrupt the OXPHOS metabolic profile. In summary, these metabolic studies show that T cells simultaneously stimulated with co-stimulatory signals undergo metabolic reprogramming with prompted OXPHOS and glycolytic activity, which might contribute to the enhanced proliferative capacity and potent cytotoxicity of T cells.

Transcriptional reprogramming of T cells through distinct TriTCE co-stimulation

We performed RNA-seq analysis of sorted T cells to investigate how the addition of co-stimulation receptor agonism enhances antitumor responses and persistence of T cells (figure 7A). Using principal component analysis, we assessed the relative relationship between the different groups of antibody-treated T cells co-cultured with target tumor cells (figure 7B). GSEA unveiled elevated cell cycle signaling pathways in TriTCE-treated T cells, suggesting sustained proliferation on antigen stimulation (figure 7C,E). Importantly, T cells treated with TriTCEs exhibited enrichment in gene signatures associated with OXPHOS metabolic processing pathways, mirroring the active metabolic reprogramming observed in seahorse assays *in vitro* (figure 7C). In addition, TriTCE-treated T cells showed higher expression of genes encoding cytotoxic molecules, including GZMB, GZMA, NKG7, GNLY, and IFNG, revealing significant enrichment in pathways

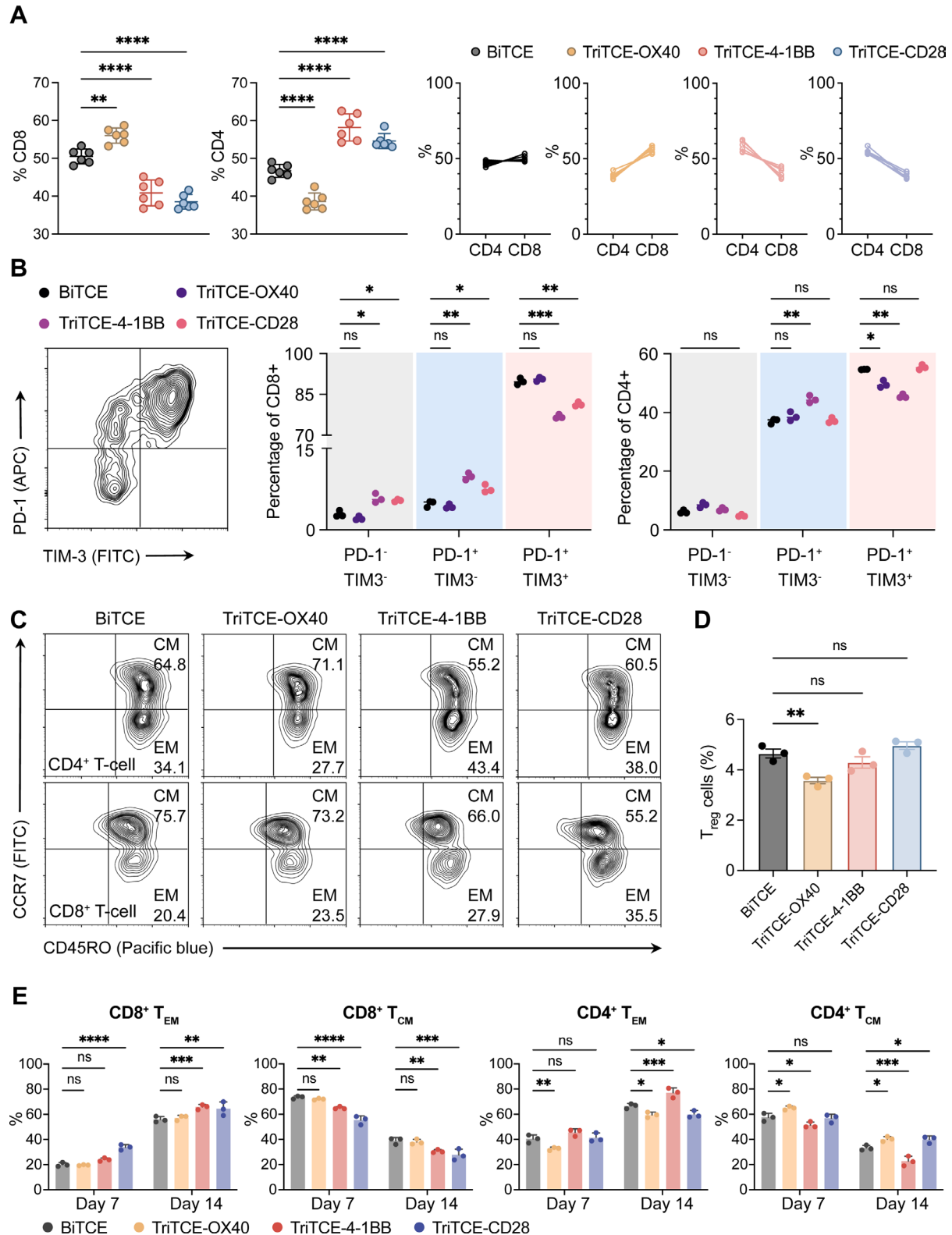


Figure 5 Distinct T-cell phenotype treated with co-stimulatory TriTCEs on tumor antigen stimulation. (A) CD8⁺ and CD4⁺ T-cell ratios in different treatment groups in the coculture assays after 48 hours were analyzed by flow cytometry (gated on CD3⁺ T cells). (B) The expression of T-cell exhaustion marker PD-1 and TIM-3 in T cells after incubation with tumor cells and either BiTCE, TriTCE-OX40, TriTCE-4-1BB, or TriTCE-CD28. (C, E) Representative flow cytometry plots of cell-surface expression of CCR7 and CD45RO (C) and quantitative results (E) showing the frequencies of central memory T-cell (T_{CM}) and effector memory T-cell (T_{EM}). (D) Percentage of CD4CD25Foxp3 Tregs in different treatment groups in the coculture assays were analyzed by flow cytometry. Data show individual values and mean±SD (n=3 independent experiments each). Statistical significance was measured by one-way ANOVA with Dunnett's post-test analysis. *p<0.05; **p<0.01; ***p<0.001; ****p<0.0001; ns, no significance compared with the bispecific control. ANOVA, analysis of variance; TriTCEs, trispecific T cell-engaging antibodies.

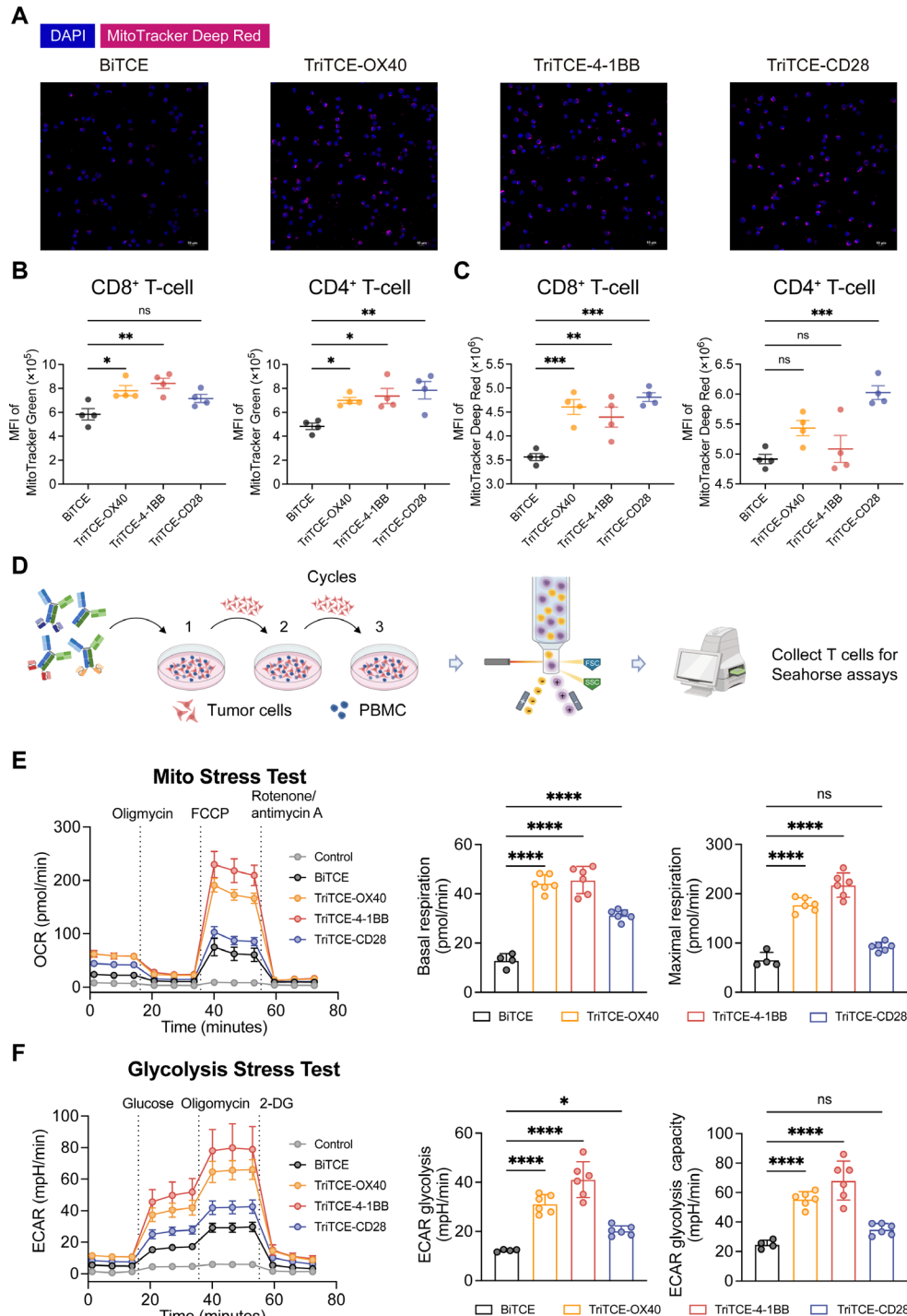


Figure 6 Co-stimulatory TriTCEs promote T-cell metabolic activities. (A) Representative confocal images stained with Mitotracker deep red (pink) and DAPI (blue). Scale bars represent 10 μ m. (B, C) Mitochondrial mass (B) and mitochondrial membrane potential (C) of CD8⁺ and CD4⁺ T cells in different treatment groups in the coculture assays analyzed by flow cytometry. (D) Schematic diagram of the Seahorse experimental design. At day 1, peripheral blood mononuclear cells (PBMCs) were added to the tumor cell-seeded plate at E:T (effector:target ratio) of 4:1 with 1 nM BiTCE, TriTCE-OX40, TriTCE-4-1BB, and TriTCE-CD28, respectively. At days 4 and 7, new tumor cells were added to the plate. At day 9, CD3⁺ T cells were sorted and collected for Seahorse assays by flow cytometry after three rounds of co-culture experiment. (E, F) Metabolic profile showing O₂ (E) and glucose consumption (F) of CD3⁺ T cells in different treatment groups after three rounds of co-culture experiment (n=6 samples). O₂ consumption rate and extracellular acidification rate were assessed at different time points in a Seahorse XF-96 analyzer. n=2 independent experiments. Summarized data on the right display basal oxygen consumption rate (OCR), maximal OCR, extracellular acidification rate (ECAR) glycolysis, and ECAR glycolysis capacity of sorted CD3⁺ T cells. Data show mean \pm SD and were analyzed by one-way ANOVA with Dunnett's post-test analysis. *p<0.05; **p<0.01; ***p<0.001; ****p<0.0001; ns, no significance compared with the bispecific control. ANOVA, analysis of variance; TriTCEs, trispecific T cell-engaging antibodies.

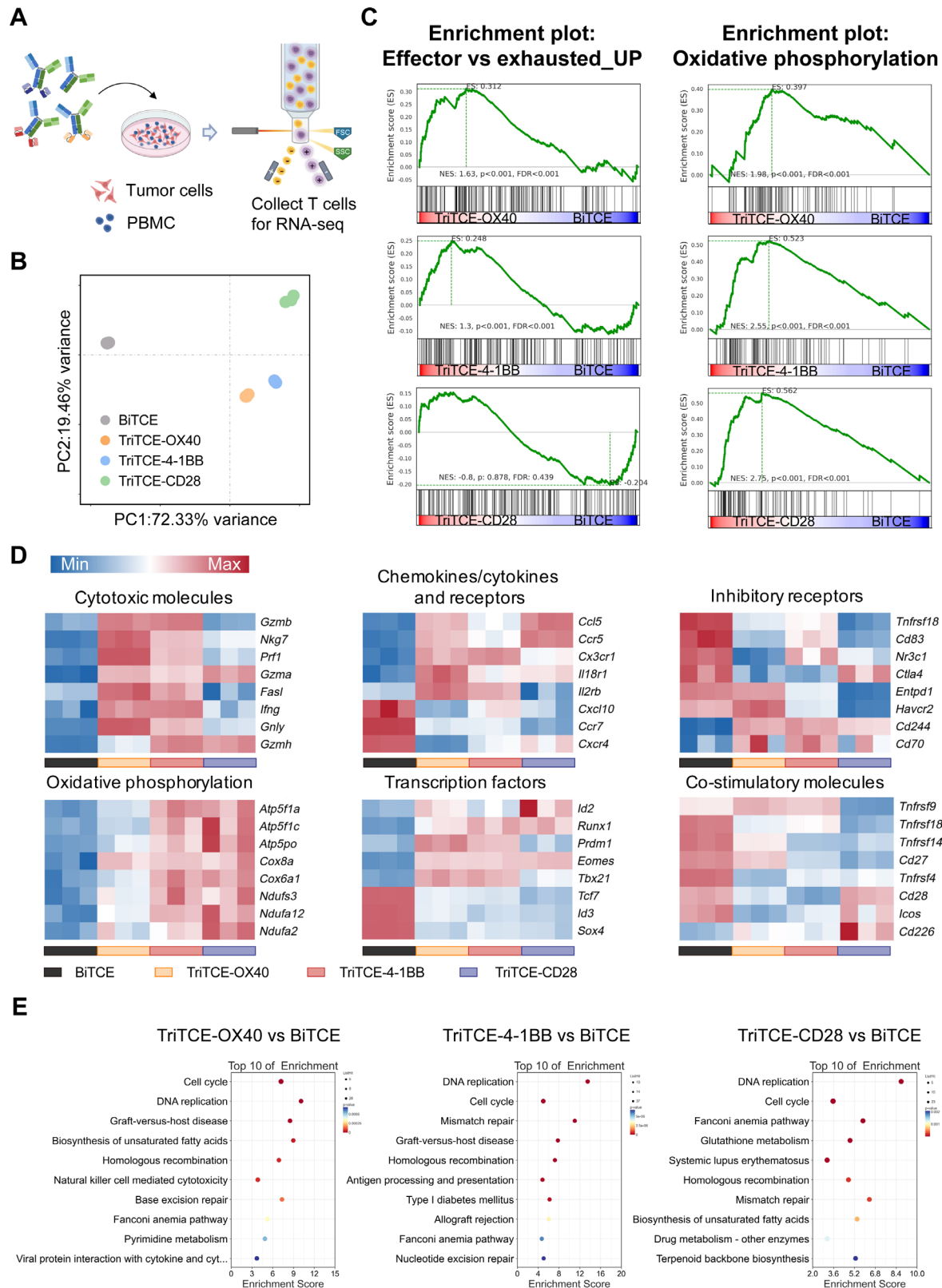


Figure 7 Transcriptional profiling of T cells co-cultured with distinct co-stimulatory TriTCEs. (A) Schematic diagram of the sample preparation for RNA-seq. Peripheral blood mononuclear cells (PBMCs) were co-cultured with tumor cells and were stimulated with 1 nM BITCE, TriTCE-OX40, TriTCE-4-1BB, and TriTCE-CD28, respectively. CD3⁺ T cells were sorted and collected for RNA-seq at day 5. (B) Principal component analysis of transcriptome data from sorted CD3⁺ T cells in different treatment groups. (C) GSEA of the effector versus exhausted UP and oxidative phosphorylation pathway genes in T cells treated with bispecific and trispecific antibodies. (D) Heat map illustrating the relative expression of genes in sorted T cells in different treatment groups from the co-culture assay. (E) Enrichment analysis of gene sets in T cells after treatment with TriTCE-OX40, TriTCE-4-1BB, and TriTCE-CD28 compared with the bispecific control is shown.

associated with T-cell effector function (figure 7D). Overall, transcriptional analysis suggested that dual targeting of CD3 and co-stimulatory receptors sustains effector function, cell proliferation signals, and metabolic fitness in T cells, translating into potent and sustained antitumor activity.

DISCUSSION

Providing optimal T-cell co-stimulation and reverse T-cell dysfunction in the TME remains a critical challenge in achieving clinical responses to solid tumor treatment.²⁶ Our results demonstrated that the fusion of the co-stimulatory signaling agonist scFvs with a bispecific antibody provided a secondary signal to potent T-cell activation, proliferation, and cytokine production, thereby boosting antitumor efficacy in advanced solid tumors. We observed that BiTCE treatment was less effective against larger solid tumors. In contrast, TriTCE treatments were potent and significantly inhibited tumor growth. Previous studies have shown that co-stimulation signaling can enhance T-cell responses by promoting cell proliferation and survival, limiting antigen-induced cell death (AICD), reversing anergy,²⁷ and subsequently improving T-cell effector functions.²⁸ By using blocking proteins targeting the OX40, 4-1BB, and CD28 pathways, we observed a dose-dependent inhibition of T-cell activation and proliferation. This finding underscores the critical role of co-stimulatory signals in determining the magnitude of the T-cell responses. However, we also observed that the inhibition effect was relatively modest, suggesting that the CD3 engagement by the TriTCE may serve as the primary driver of T-cell activation. The results highlight the complexity of T-cell responses initiated by TriTCEs, where co-stimulatory signals and direct TCR activation signals work in concert to fine-tune the immune response.

Furthermore, we have uncovered that different choices of co-stimulation signaling triggered by TriTCEs can impact the subsequent fate of T cells. We conducted a side-by-side comparison of T-cell phenotypes in a co-culture setting with tumor cells and TriTCEs. Memory T-cells correlate positively with long-term antitumor responses.²⁹ Our results illustrated that the TriTCE-4-1BB and TriTCE-CD28 groups maintained a larger number of effector memory T cells in the cell expansion pool, whereas the TriTCE-OX40 group showed increased CD4⁺ central memory T cells. In addition, we observed that TriTCE-OX40 treatment induced fewer CD4⁺Foxp3⁺ regulatory T cells (T_{regs}), which are known to have potent suppressor functions in the TME. This finding aligns with those of previous studies showing that OX40 co-stimulation turns off the induction of new Tregs.³⁰ We found that TriTCE-OX40 treatment-induced T cells enriched the natural killer-mediated cytotoxicity signaling pathway, consistent with a report of combined therapy with OX40 agonism and PD-L1 checkpoint blockade.³¹

One major obstacle to T-cell-engaging therapies in treating solid tumors is T-cell dysfunction in the

immunosuppressive TME.³² Growing evidence indicates that T cells undergo metabolic insufficiency in the TME.³³ To mimic the solid tumor environment, we used a chronic antigen exposure model and explored the metabolic profiles of T cells stimulated with OX40, 4-1BB, or CD28 agonist TriTCEs. Of note, we found that TriTCEs actively reprogram T cell metabolism toward higher OXPHOS when there is persistent antigen stimulation. The enhanced OXPHOS observed with TriTCEs could be due to the elevated bioenergetic demands for the maintenance of long-term T-cell function, an inherently energy-intensive process, which is similar to previous studies that have underscored the metabolic enhancement in T cells.^{34 35} Notably, TriTCE-4-1BB treatment of T cells showed the best metabolic patterns, indicating its long-term efficacy in vivo. Our study provides evidence of plasticity in T-cell metabolic reprogramming induced by co-stimulatory TriTCEs. By extension, our findings suggest that integrating various co-stimulation signaling modules into a single antibody construct may reprogram T cells to meet the metabolic demands required for enhanced T cell proliferation within solid tumors.

Despite their promising potential, trispecific TCEs present several limitations that warrant further investigation and refinement. The complexity of their multivalent format poses challenges in manufacturing and quality control, potentially impacting scalability and consistency. Another significant challenge lies in translating encouraging preclinical results into clinical efficacy while maintaining an acceptable safety profile. The durability of therapeutic responses and the need for repeated administrations to sustain clinical benefits also remain areas for further study.³⁶ Additionally, striking the right balance between potency and safety is essential for the successful clinical application of trispecific TCEs.

In summary, we designed co-stimulatory specific T-cell-engager antibodies that effectively activate T cells to kill solid tumors. Compared with direct TCR stimulation, incorporating co-stimulatory signals can significantly enhance both the potency and duration of T-cell-mediated antitumor responses. Integrating multiple specificities into a single-antibody approach may expand the scope of cancer immunotherapy by allowing for the engagement of immune cells beyond T cells. This adaptable platform may facilitate the discovery of well-tolerated, off-the-shelf biological candidates to meet clinical needs.

Correction notice This article has been corrected since it was first published online. The funding statement has been updated.

Acknowledgments We thank Yingying Huang and Xin Shen from the Core Facilities of the Zhejiang University School of Medicine for their technical support.

Contributors YS: Investigation, acquisition of data, writing of the original draft. LZ: Development of methodology. XG: Formal analysis. JZ: Formal analysis. LP: Conceptualization, resources, funding acquisition, project administration, writing, review, and editing. LP is the guarantor.

Funding This study was supported by the National Natural Science Foundation of China (Grant No. 82473824 and 82073750), the National Key Research and Development Program of China (Grant No. 2023YFC3403900), and the Joint Funds of the National Natural Science Foundation of China (Grant No. U20A20409), State

Key Laboratory for Diagnosis and Treatment of Infectious Diseases (Grant No. zz202303).

Competing interests No, there are no competing interests.

Patient consent for publication Not applicable.

Ethics approval Animal experiments were approved by the Laboratory Animal Welfare and Ethics Committee of Zhejiang University (reference number 20664) and were performed in accordance with the National Institutes of Health Guide for the Care and Use of Laboratory Animals.

Provenance and peer review Not commissioned; externally peer reviewed.

Data availability statement All data relevant to the study are included in the article or uploaded as supplementary information.

Supplemental material This content has been supplied by the author(s). It has not been vetted by BMJ Publishing Group Limited (BMJ) and may not have been peer-reviewed. Any opinions or recommendations discussed are solely those of the author(s) and are not endorsed by BMJ. BMJ disclaims all liability and responsibility arising from any reliance placed on the content. Where the content includes any translated material, BMJ does not warrant the accuracy and reliability of the translations (including but not limited to local regulations, clinical guidelines, terminology, drug names and drug dosages), and is not responsible for any error and/or omissions arising from translation and adaptation or otherwise.

Open access This is an open access article distributed in accordance with the Creative Commons Attribution Non Commercial (CC BY-NC 4.0) license, which permits others to distribute, remix, adapt, build upon this work non-commercially, and license their derivative works on different terms, provided the original work is properly cited, appropriate credit is given, any changes made indicated, and the use is non-commercial. See <http://creativecommons.org/licenses/by-nc/4.0/>.

ORCID iDs

Yanping Sun <http://orcid.org/0009-0004-3401-917X>

Linling Zhou <http://orcid.org/0009-0008-0306-3441>

Xinyu Gu <http://orcid.org/0009-0009-1253-3772>

Jiaqi Zhao <http://orcid.org/0009-0004-5616-0342>

Jie Bi <http://orcid.org/0009-0003-8890-5436>

Liqiang Pan <http://orcid.org/0000-0002-6557-8351>

REFERENCES

- Cappell KM, Kochenderfer JN. Long-term outcomes following CAR T cell therapy: what we know so far. *Nat Rev Clin Oncol* 2023;20:359–71.
- Sharma P, Goswami S, Raychaudhuri D, et al. Immune checkpoint therapy-current perspectives and future directions. *Cell* 2023;186:1652–69.
- Stultz J, Fong L. How to turn up the heat on the cold immune microenvironment of metastatic prostate cancer. *Prostate Cancer Prostatic Dis* 2021;24:697–717.
- Goebeler ME, Bargou RC. T cell-engaging therapies - BITEs and beyond. *Nat Rev Clin Oncol* 2020;17:418–34.
- Hou AJ, Chen LC, Chen YY. Navigating CAR-T cells through the solid-tumour microenvironment. *Nat Rev Drug Discov* 2021;20:531–50.
- Philip M, Schietinger A. CD8+ T cell differentiation and dysfunction in cancer. *Nat Rev Immunol* 2022;22:209–23.
- Binnewies M, Roberts EW, Kersten K, et al. Understanding the tumor immune microenvironment (TIME) for effective therapy. *Nat Med* 2018;24:541–50.
- Esensten JH, Helou YA, Chopra G, et al. CD28 Costimulation: From Mechanism to Therapy. *Immunity* 2016;44:973–88.
- Chester C, Sanmamed MF, Wang J, et al. Immunotherapy targeting 4-1BB: mechanistic rationale, clinical results, and future strategies. *Blood* 2018;131:49–57.
- Yadav R, Redmond WL. Current Clinical Trial Landscape of OX40 Agonists. *Curr Oncol Rep* 2022;24:951–60.
- Mayes PA, Hance KW, Hoos A. The promise and challenges of immune agonist antibody development in cancer. *Nat Rev Drug Discov* 2018;17:509–27.
- Belmontes B, Sawant DV, Zhong W, et al. Immunotherapy combinations overcome resistance to bispecific T cell engager treatment in T cell-cold solid tumors. *Sci Transl Med* 2021;13:eabd1524.
- Suntharalingam G, Perry MR, Ward S, et al. Cytokine storm in a phase 1 trial of the anti-CD28 monoclonal antibody TGN1412. *N Engl J Med* 2006;355:1018–28.
- Segal NH, Logan TF, Hodi FS, et al. Results from an Integrated Safety Analysis of Urelumab, an Agonist Anti-CD137 Monoclonal Antibody. *Clin Cancer Res* 2017;23:1929–36.
- Bander NH, Trabulsi EJ, Kostakoglu L, et al. Targeting metastatic prostate cancer with radiolabeled monoclonal antibody J591 to the extracellular domain of prostate specific membrane antigen. *J Urol* 2003;170:1717–21.
- Xu D, Alegre ML, Varga SS, et al. In vitro characterization of five humanized OKT3 effector function variant antibodies. *Cell Immunol* 2000;200:16–26.
- Min J, Wu Y, Finn RF, et al. Binding molecules to the human ox40 receptor. Google Patents; 2011.
- Beyersdorf N, Gaupp S, Balbach K, et al. Selective targeting of regulatory T cells with CD28 superagonists allows effective therapy of experimental autoimmune encephalomyelitis. *J Exp Med* 2005;202:445–55.
- Akamatsu Y, Wang J. Anti-4-1bb antibodies and their uses. Google Patents; 2020.
- Love MI, Huber W, Anders S. Moderated estimation of fold change and dispersion for RNA-seq data with DESeq2. *Genome Biol* 2014;15.
- Subramanian A, Tamayo P, Mootha VK, et al. Gene set enrichment analysis: A knowledge-based approach for interpreting genome-wide expression profiles. *Proc Natl Acad Sci USA* 2005;102:15545–50.
- Komai T, Inoue M, Okamura T, et al. Transforming Growth Factor-β and Interleukin-10 Synergistically Regulate Humoral Immunity via Modulating Metabolic Signals. *Front Immunol* 2018;9:1364.
- Blank CU, Haining WN, Held W, et al. Defining 'T cell exhaustion'. *Nat Rev Immunol* 2019;19:665–74.
- Falcomatà C, Bärthel S, Schneider G, et al. Context-Specific Determinants of the Immunosuppressive Tumor Microenvironment in Pancreatic Cancer. *Cancer Discov* 2023;13:278–97.
- Togashi Y, Shitara K, Nishikawa H. Regulatory T cells in cancer immunosuppression - implications for anticancer therapy. *Nat Rev Clin Oncol* 2019;16:356–71.
- Hirz T, Mei SL, Sarkar H, et al. Dissecting the immune suppressive human prostate tumor microenvironment via integrated single-cell and spatial transcriptomic analyses. *Nat Commun* 2023;14:66310.
- Wilcox RA, Tamada K, Flies DB, et al. Ligation of CD137 receptor prevents and reverses established anergy of CD8+ cytolytic T lymphocytes in vivo. *Blood* 2004;103:177–84.
- Taraban VY, Rowley TF, O'Brien L, et al. Expression and costimulatory effects of the TNF receptor superfamily members CD134 (OX40) and CD137 (4-1BB), and their role in the generation of anti-tumor immune responses. *Eur J Immunol* 2002;32:3617–27.
- Gebhardt T, Park SL, Parish IA. Stem-like exhausted and memory CD8+ T cells in cancer. *Nat Rev Cancer* 2023;23:780–98.
- Vu MD, Xiao X, Gao W, et al. OX40 costimulation turns off Foxp3+ Tregs. *Blood* 2007;110:2501–10.
- van der Sluis TC, Beyrend G, van der Gracht ETI, et al. OX40 agonism enhances PD-L1 checkpoint blockade by shifting the cytotoxic T cell differentiation spectrum. *Cell Rep Med* 2023;4:100939.
- Thommen DS, Schumacher TN. T Cell Dysfunction in Cancer. *Cancer Cell* 2018;33:547–62.
- Franco F, Jaccard A, Romero P, et al. Metabolic and epigenetic regulation of T-cell exhaustion. *Nat Metab* 2020;2:1001–12.
- Guo Y, Xie Y-Q, Gao M, et al. Metabolic reprogramming of terminally exhausted CD8+ T cells by IL-10 enhances anti-tumor immunity. *Nat Immunol* 2021;22:746–56.
- Hirabayashi K, Du H, Xu Y, et al. Dual Targeting CAR-T Cells with Optimal Costimulation and Metabolic Fitness enhance Antitumor Activity and Prevent Escape in Solid Tumors. *Nat Cancer* 2021;2:904–18.
- Philipp N, Kazerani M, Nicholls A, et al. T-cell exhaustion induced by continuous bispecific molecule exposure is ameliorated by treatment-free intervals. *Blood* 2022;140:1104–18.